Journal of the European Ceramic Society **16** (1996) 1377–1383

PII: S0955-2219(96)00060-X
0955-2219/96/$15.00

Estimating Tensile Creep Rate of Ceramics from Flexure Data

Dong-Joo Lee

Department of Mechanical Engineering, Yeungnam University, Gyungsan, Gyungbuk, Korea

(Received 18 April 1994; revised version received 4 March 1996; accepted 14 March 1996)

Abstract

A new model of ceramic creep in four-point bending is proposed to determine the creep rate that corresponds to tensile creep at an elevated temperature. Based on the assumption that ceramics creep only in tension and there is no creep in compression, the tensile creep rate which is invariant with time in the secondary mode is calculated in a simple way. Since the initially applied maximum tensile stress does not correspond to the stress at the secondary creep range, the creep-induced stress at the time of measurement is calculated based on beam deflection. Then, the calculated tensile creep rates from four-point bending data are compared with observed tensile creep rates for both an alumina ceramic at 1000°C and a silicon nitride ceramic at 1200°C. This study shows the usefulness of flexural creep tests not only to verify the accuracy of tensile creep tests, but also to obtain the tensile creep data in a less expensive and easier way. © 1996 Elsevier Science Limited

Introduction

A knowledge of the creep behaviour of ceramic materials is of importance in computing their lifetime at high temperatures. For brittle ceramic materials, the power-law creep parameters are commonly deduced from load–point displacement data generated by four-point bend experiments under the assumption that tensile and compressive behaviours obey the same constitutive law. However, because of the microcracking and cavitation that occur preferentially under tension, it is now well recognized[1,2] that this premise may not always be valid. Also, bend data reflect a combination of tensile and compressive responses, so individual effects of creep deformation and damage evolution cannot be distinguished readily. The real stress/strain in a flexural creep test cannot be calculated properly unless an evaluation of the creep parameters describing compressive and tensile creep is considered. Therefore, flexural creep measurements for ceramic materials are easy to perform, but difficult to analyse.

For reasons of simplicity and economy, however, ceramic tensile responses are evaluated by bend tests.[3,4] There are also rigorous efforts to estimate the uniaxial creep behaviour.[1,5] But the flexural creep tests have been analysed by the method of Hollenberg *et al.*,[6] who assumed that the neutral axis is the midplane of the flexure specimen. This approach was widely used to interpret and calculate the ceramic creep versus stress as if compressive and tensile creep behaved symmetrically in ceramic materials.[3,7]

Chuang[5] analysed flexural creep for materials whose compressive and tensile creep behaviours are not symmetrical. Using the power-law function of stress to present the strain rate in secondary creep, he presented the two governing equations to derive the location of the neutral axis of a beam under bending as related to the curvature rate. That axis does not pass through the centroid of the beam's cross-section. To solve complicated functions, he adopted an approximation method of double integration to estimate the variation of the neutral axis curvature. As pointed out by Krause,[8] Chuang's analysis is awkward to execute and its accuracy is limited to the size of the incremental step in the curvature rate generated in his approximation. Also, experimental implementation to measure accurately the curvature is extremely difficult. Therefore, many researchers[9,10] measured the creep behaviour of ceramic materials using the method of Hollenberg *et al.*[6] until recently, even though such calculations involve error if the materials behave differently in compressive and tensile creep. Indeed, Ferber *et al.*[9] found that the compressive and tensile creep properties are not symmetrical by measuring directly the compressive and tensile properties of the same material. However, they proceeded to predict values of flexural strain and flexural creep rate using the relation

that the midplane of the specimen is the neutral axis of strain. Frett *et al.*[11] also investigated the creep behaviour of a ceramic in four-point bend tests and showed the relations between the local creep state in transient and stationary creep ranges and the global deformation. They also concluded that stationary creep under compressive stresses must be negligible.

The objectives of this study are to offer a simple analytical model to estimate the tensile creep rate from four-point bending data. By introducing certain hypotheses on the creep and subsequent mathematical modelling of the situation, the experimental creep data of Ferber *et al.*[9] are recalculated and then the measured tensile creep rate is compared with the calculated tensile creep rate. Various aspects of these results are discussed. This study not only shows the usefulness of flexural creep tests to verify the accuracy of tensile creep tests, but also provides a simple way to calculate tensile creep rate during the secondary mode of creep in flexure without using the compressive and tensile properties of the same material.

A Simplified Model of Tensile Creep During Four-Point Bending

As is evident from an analysis of relevant literature,[3,8] most ceramic materials creep in tension much more easily than in compression. The presence of such creep micromechanisms as growth of pores or grain boundary sliding accounts for the difference. Recently, Frett *et al.*[11] concluded that stationary creep under compressive stresses must be negligible by measuring the expansion of the specimen after the creep test. By assuming the absence of creep in compression, this can be implemented into a model considering the limiting case and, in order to obtain a simple closed-form solution, two major assumptions are made:

(1) the material creeps only in tension and there is no creep in compression; and
(2) stress is distributed across the extended part of the cross-section as shown in Fig. 1.

Then, according to existing experimental data, the strain rate ($\dot{\varepsilon}_t$) dependence on the tensile stress (σ_t) can be approximated by a power law in the steady state as

$$\dot{\varepsilon}_t = \alpha \sigma_t^{\beta} \tag{1}$$

where α and β are the material constants and β is always >1. The creep in a flexed beam is more intensive in the volumes of material closer to the tensile surface of the beam where the stresses are higher, as shown in Fig. 1. The redistribution of stresses takes place during the initial period of creep, with a tendency to level the stress across the portion of the cross-section in tension. A rather complex computer simulation of the process of stress redistribution (Fig. 2) is published in the literature.[12] It is clear that eventually this redistribution can be approximated by a simpler one as shown in Fig. 1.

The model relationships are obtained on the basis of the following considerations. First, the central section of the beam is in pure bending; therefore, the cross-sections which were plane before deformation remain plane after deformation

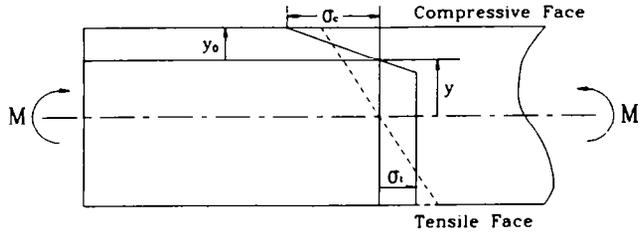

Fig. 1. Stress distribution due to bending.

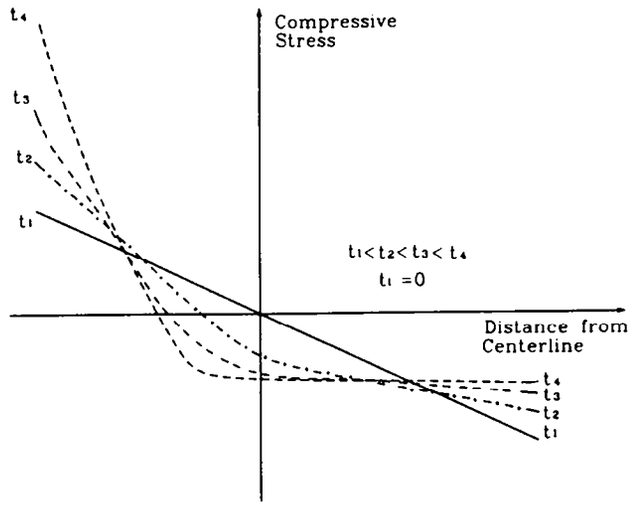

Fig. 2. Bending-stress redistribution at increasing times: t_1, t_2, t_3 and t_4 (Ref. 12).

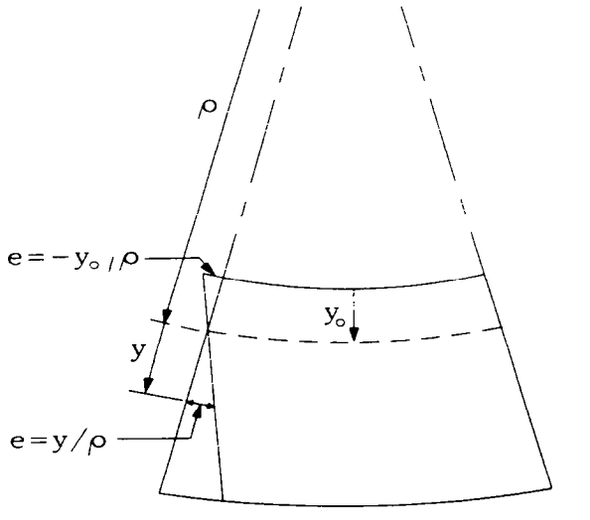

Fig. 3. Segment of a bent beam.

including creep. These sections rotate against the neutral plane, the position of which is defined by an ordinate y_0 from the outer compressed surface of the beam. A beam has a rectangular cross-section. The total beam height is h and its width is b (Fig. 3). The ordinate y_0 which before creep initiation is $y_0 = h/2$ becomes $y_0 < h/2$ and shifts monotonically towards the outer compression surface as the volumes in tension proceed to creep. A layer of the beam at distance y from the neutral layer (Fig. 3) experiences the total strain as

$$e = y/\rho \tag{2}$$

where ρ is the radius of the beam curvature. From the assumption on the absence of creep in compression and eqn (2) follows an expression for the maximum stress in compression

$$\sigma_c = Ey_0/\rho \tag{3}$$

Two equations for the balance of external forces and internal stresses in cross-section F are

$$\int_F \sigma dF = 0 \tag{4a}$$

$$\int_F y\sigma dF = M \tag{4b}$$

These can be used to establish a relationship between σ_t, the uniformly distributed tensile stress; y_0, the position of the neutral plane; M, the applied moment; and ρ, the radius of curvature. One additional assumption, when writing out the integrals in eqns (4a) and (4b), simplifies the expressions while introducing negligible imprecision for the case of well developed creep. Namely, one assumes that the tensile stress, σ_t, is distributed uniformly across the whole area in tension and not as shown in Fig. 1. The difference in calculation of integrals (4a) and (4b) is small if a well developed state of creep is considered and the area where σ_t changes is small. Then, expression (4a) can be written as

$$\sigma_t (h - y_0)b = \sigma_c y_0 b/2 \tag{5}$$

Similarly, for expression (4b) as

$$\sigma_t(h - y_0)^2 b/2 + \sigma_c y_0^2 b/3 = M \tag{6}$$

By substituting eqn (2) for eqns (5) and (6), one obtains

$$\sigma_t(h - y_0) = Ey_0^2/2\rho \tag{7}$$

and

$$\sigma_t(h - y_0)^2/2 + Ey_0^3/3\rho = M/b \tag{8}$$

Expressing σ_t from eqn (7) as

$$\sigma_t = \frac{Ey_0^2}{2(h - y_0)\rho} \tag{9}$$

and substituting for eqn (8), one obtains a cubic algebraic equation with respect to an unknown y_0 as follows

$$y_0^3 + 2h\, y_0 = 12M\rho/bE \tag{10}$$

The radius of curvature, ρ, can be found as a function of the measured displacement, Δ (see Fig. 4), as

$$\rho = L\, L_1/2\Delta \tag{11}$$

where L and L_1 are the lengths of outer and inner spans, respectively. If one assumes that the areas outside the inner span do not creep, eqns (10) and (11) allow one to find y_0 as a function of M, Δ, E and the specimen geometry. Then, σ_t is found from eqn (9). The corresponding strain rate can be found by using an expression for the maximum tensile strain

$$e_{max} = (h - y_0)/\rho \tag{12}$$

Since e_{max} consists of two components, elastic and creep,

$$e_{max} = e^e_{max} + e^c_{max} \tag{13}$$

Since the elastic one is $e^e_{max} = \sigma_t/E$ and the creep component is e_c, one then can write it as

$$\sigma_t/E + e_c = (h - y_0)/\rho \tag{14}$$

By differentiation of eqn (14) with respect to time, one can find

$$\dot{\sigma}_t/E + \dot{e}_c = -\dot{y}_0/\rho - (h - y_0)\,\dot{\rho}/\rho^2 \tag{15a}$$

from which

$$\dot{e}_c = -\dot{\sigma}_t/E - \dot{y}_0/\rho - (h - y_0)\,\dot{\rho}/\rho^2 \tag{15b}$$

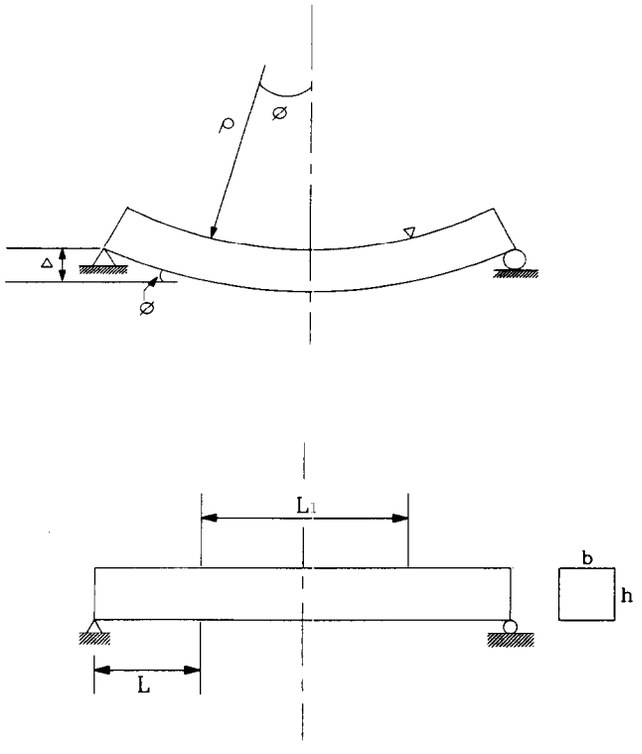

Fig. 4. Specimen geometry and deformed beam in bending.

For calculation of $\dot{\epsilon}_c$, the derivatives ρ, y_0 and σ_t in eqn (15b) can be expressed in terms of displacement rate, $\dot{\Delta}$. From eqn (11)

$$\dot{\rho} = -L\,L_1\dot{\Delta}/2\Delta^2 \tag{16}$$

By solving eqns (10) and (11), a relationship between y_0 and Δ can be established. The calculated function $y_0 = y_0(\Delta)$ is graphically presented in Fig. 5 in ln y_0 versus ln Δ coordinates for the cases of different values of modulus. The ln y_0 versus ln Δ function turned out to be linear in the range of well developed creep, i.e. ln $y_0 = k$ ln Δ + ln c where slope $k = -0{\cdot}9$ for $E = 400$ GPa, $k = -0{\cdot}88$ for $E = 300$ GPa and $k = -0{\cdot}77$ for $E = 210$ GPa. Then, the derivative y_0 can be analytically expressed through Δ as

$$\dot{y}_0 = y_0 k\dot{\Delta}/\Delta \tag{17}$$

From eqn (9), one obtains

$$\dot{\sigma}_t = -\frac{y_0^2 E}{2\Delta\rho(h-y_0)}\left[\frac{L\,L_1\dot{\Delta}}{2\Delta\rho} + \frac{(2h-y_0)k\dot{\Delta}}{(h-y_0)}\right] \tag{18}$$

By substituting eqns (16), (17) and (18) for eqn (15), one obtains the following expression for $\dot{\epsilon}_c$ in terms of $\dot{\Delta}$, y and ρ:

$$\dot{\epsilon}_c = \frac{\dot{\Delta}}{LL_1}\left[(h-y_0) - 2ky_0 - \frac{y_0^2}{(h-y_0)}\left(1+\frac{(2h-y_0)k}{(h-y_0)}\right)\right] \tag{19}$$

Discussion

In order to compare the measured tensile creep rate with the calculated tensile creep rate from four-point bending data, the model described in the previous section is applied. Ferber *et al.*[9] measured the creep rate of commercially available Al_2O_3 (AD94, Coors Ceramics, Golden, CO) at 1000°C and Si_3N_4 (SN220M Kyocera American Inc., Des Plains, IL) at 1200°C using tension, compression and flexure specimens. They found a pronounced difference in the creep deformation behaviours measured in tension and compression for both ceramics. They also found a general agreement between the flexural creep data and the predicted data from existing creep deformation models. In their paper they also used Chuang's method[5] to predict the stress dependence of the neutral axis location and specimen midspan displacement rate from the tension and compression data. But, they improperly calculated flexural creep strains directly from load–displacement rate data by assuming that the midplane of the specimen was the neutral axis of strain. Therefore, their comparison of flexural creep strain rates from the respective compression and tension tests was questionable.

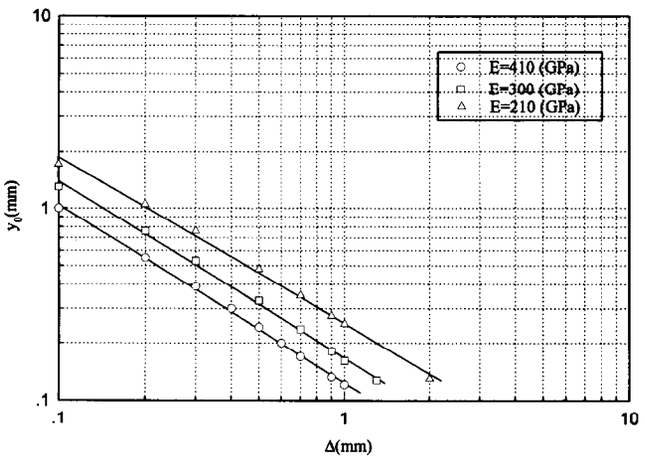

Fig. 5. Position of neutral axis as a function of modulus.

In this study, it is clear from the assumption on stress distribution (see Fig. 1) that the model should be applied only when the creep deformation reaches an advanced stage of creep. To calculate the tensile creep rate from experimental creep data under flexural loading, the measured flexural creep rate and the deflection rate should be recalculated from the data of Ferber *et al.*[9] Also, the displacement at the loading point is needed from their displacement at the centre of the sample relative to the inner load points. Then the calculated tensile creep rate according to the model described in the previous section can be compared with the experimentally measured tensile creep rate of Ferber *et al.*[9]

From the measured flexural creep rate ($\dot{\epsilon}_{max}$), the deflection rate, $\dot{\Delta}_r$, at the centre of the beam relative to the two inner load points can be calculated from a simple relation as

$$\dot{\epsilon}_{max} = 4\,h\,\dot{\Delta}_r/L_1^2 \tag{20}$$

Then, the deflection rate at the loading point is obtained from eqn (11) as

$$\dot{\epsilon}_{max} = h/2\dot{\rho} = h\dot{\Delta}/LL_1 \tag{21}$$

From the two relations and $L_1 = 2L$, one can obtain $\dot{\Delta} = 2\dot{\Delta}_r$ and similarly $\Delta = 2\Delta_r$. From the curve of creep strain for AD94 alumina measured in flexure (Fig. 4(c) in Ref. 9), the deflection at 40 h as steady-state creep in the secondary mode is calculated from the above relations. The predicted values of neutral axis position are obtained from Fig. 5 with the measured displacement. In this study, modulus values of 350 and 300 GPa are used for AD94 alumina and SN220M silicon nitride, respectively. The top half of Table 1 summarizes the experimentally obtained creep strain, displacement rate, beam deflection after 40 h of creep and values of neutral axis location associated with flexure loading. Using the above data and eqn (19), the tensile creep rate for AD94 is calculated. The lower half of Table 1 shows the same

values for SN220M after 80 h of creep. Flexural creep data of higher stress, where the material typically failed in the range of transient creep, are not used in this calculation for both materials.

In order to compare the measured tensile creep rate, invariant with time in the secondary mode of creep, with the calculated tensile creep rate from the flexural creep test, the corresponding tensile stress at the time of measurement should first be calculated. Since there is considerable stress relaxation during the creep test especially after a large deflection, it is not adequate to compare the tensile creep rate with an initial maximum applied stress. Therefore, the creep-induced stresses at the time of measurement are needed to compare with the experimental data under tensile loading. The corresponding tensile stress can be calculated from simple elastic beam theory, but considering the change of neutral axis. Since the equilibrium of the forces acting on the cross-section can be expressed by strain (ϵ) as $dF = b dy$ and $\epsilon = y/\rho$, the equilibrium equations can be written from eqn (4a) as

$$\int_{-\epsilon_c}^{\epsilon_t} f(\epsilon) d\epsilon = 0 \tag{22}$$

and from eqn (4b) as

$$\int_{-\epsilon_c}^{\epsilon_t} f(\epsilon)\epsilon d\epsilon = M(\epsilon/y)^2/b \tag{23}$$

By differentiating with respect to the curvature using Leibnitz's rule, one can obtain the outer maximum tensile stress

$$\sigma_t = \frac{\dot{M}(\epsilon + \epsilon_c) + 2M(\dot{\epsilon}_t + \dot{\epsilon}_c)}{h^2\dot{\epsilon}_t} \tag{24}$$

For a small deflection of the beam under a static bending test, the change of moment is assumed to be zero. Then one can rearrange eqn (24), since $\epsilon_t = (h - y_0)/\rho$ and $\epsilon_c = y_0/\rho$, from eqns (16) and (17) as

$$\sigma_t = \frac{FL}{h[(h - y_0) - ky_0]} = \frac{2M}{bh[(h - y_0) - ky_0]} \tag{25}$$

Assuming that the initial strain prior to creep deformation is linear elastic, the initial stress (σ_i) that exists on the tension side is defined by

$$\sigma_i = 6M/bh^2 \tag{26}$$

After obtaining the applied moment from the initially applied stresses and using the data in Table 1, the creep-induced stresses (σ_t) at the time of measurement are obtained and shown in Table 2. Then the tensile creep rate is calculated using eqn (19) in the previous section. Figures 6 and 7 show the predicted stress dependence of tensile creep rates for AD94 alumina and SN220M silicon nitride, respectively, compared with experimental data. Even though the calculated tensile creep rates are not exactly as the measured data, the figures show reasonable fit for both ceramics. Considering the original strain analysis is done from a simple elastic relation for small deflection, the values of displacement and displacement rate may be different. The

Table 2. Applied moment, calculated creep-induced stress and predicted stress values by Ferber *et al.*[9] associated with flexure loading

	σ (*MPa*)	M (*N mm*)	σ_t (*MPa*)	σ_f (*MPa*)
AD94 Alumina	80	480	26·9	39·0
	60	360	22·8	31·5
	50	300	17·4	27·5
SN220M Silicon Nitride	80	480	33·42	40·6
	60	360	25·3	32·2
	50	300	20·6	27·0

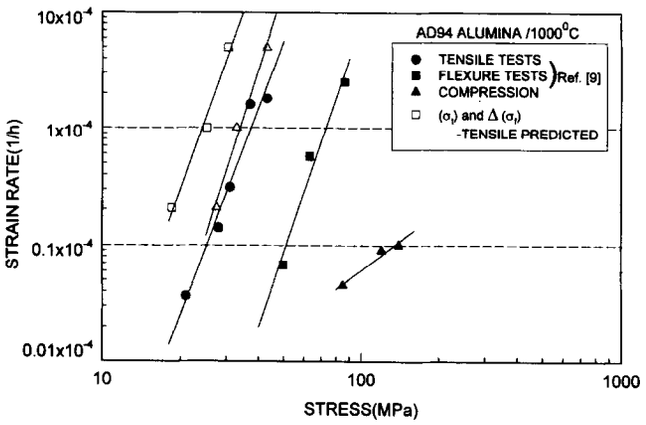

Fig. 6. Stress dependence of creep rate for AD94 alumina at 1000°C.

Table 1. Elastic stress, measured creep strain, displacement rate at measuring point and loading point, predicted neutral position and steady state creep rate associated with flexure loading.

	σ (*MPa*)	$\dot{\epsilon}$ ($^{-1}$) ($\times 10^{-4}$)	$\dot{\Delta}_r$ (*mm h*$^{-1}$)	$\dot{\Delta}$ (*mm*)	y_0 (*mm*)	Δ (*mm*)	$\dot{\epsilon}_c^{-1}$ ($\times 10^{-4}$)
AD94 Alumina	80	2·50	0·0094	0·0188	0·35	0·3	5·02
	60	0·57	0·0020	0·0040	0·4	0·29	1·07
	50	0·069	$2·0 \times 10^{-4}$	$4·0 \times 10^{-4}$	1·5	0·07	0·22
SN220M Silicon Nitride	99	3·50	0·0106	0·0212	0·38	0·5	5·62
	77	1·6	0·00555	0·0111	0·37	0·45	3·06
	60	1·0	0·00347	0·0069	0·52	0·3	2·00

modulus values used in the calculation might not be the same as those of the tested materials, even though changes can be small. Also, it is difficult to measure accurately the creep rate of ceramic materials at high temperature. These can be the sources of a small discrepancy as shown in Figs 6 and 7.

The creep-induced stress along the tensile surface of the flexure samples was calculated by Ferber *et al.*[9] using estimated values of the material constants α and β for both compression and tension, the location of the neutral axis and the predicted flexural creep strain rate as given in their eqns (5a) and (5b). Table 2 shows a comparison between the creep-induced stresses (σ_f) obtained by Ferber *et al.*[9] and σ_t from eqn (25). The stress drop associated with the effect of the creep-induced stress relaxation is large, as shown in Table 2, the values obtained by eqn (25) being a little more severe than the values obtained by Ferber *et al.*[9] However, the values of tensile creep rate obtained from σ_f show the better fit than the creep data obtained from σ_t by eqn (25) when compared with experimental tensile data, as shown in Figs 6 and 7. But their analysis involved not only using the questionable predicted values, but also experimental data of tension and compression, and time-consuming calculation. Therefore, the use of their predicted values should be reconsidered. However, one needs more experimental data of creep — tensile and flexural — on the same materials to verify the relations between σ_t and σ_f. Ferber *et al.*[9] tried to verify this stress relaxation by measuring the short-term strength of samples before and after creep testing at high temperature. The systematic tests of this kind can be useful to verify it. However, the creep-induced tensile stress calculated using eqn (25) is simple and does not involve the use of estimated and experimental values under compression and tension. Frett *et al.*[11] also tried to obtain the creep-induced tensile stress as a function of time after loading, but there is a strange hump around 10 h of loading and so their results are not compared with data of this work. In a previous paper,[13] the creep rates of six ceramics were measured in four-point bending at 1100°C and the tensile creep rate was calculated. Using those data and the tensile creep rate of these ceramics, the creep-induced stress will be discussed elsewhere in detail.

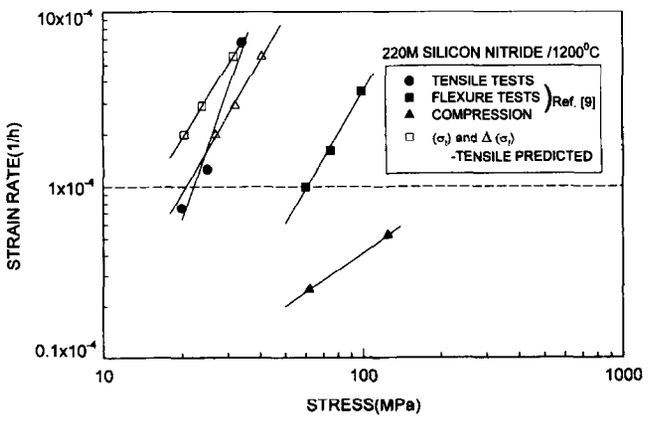

Fig. 7. Stress dependence of creep rate for SN 220M silicon nitride at 1200°C.

Recently, Krause[8] recalculated experimental data of Ref. 9 to compare the observed and theoretical values of the normalized curvature rate versus bending moment, and concluded that stresses and strains during secondary creep tests in flexure cannot be properly calculated unless an evaluation of the compressive and tensile creep properties is appropriately considered. Flexural creep tests, however, can be used to verify the accuracy of tensile creep tests on a material. This analysis shows the way to determine the tensile creep behaviour of a material using the flexural creep test in a simple way. Since ceramics do creep in compression, a new model considering the influence of compressive creep, even though it will be extremely small, will be developed.

For more accurate and easier testing of ceramic creep in four-point bending as mentioned by Hollenberg *et al.*,[6] it is believed that use of the three probes required in measuring Δ_r deflections at three points is more complex and prone to experimental difficulties than the two-probe scheme used in this work. If there is a limitation of any kind and one needs tensile creep data, then as an alternative way that is less expensive and easier to perform, a simple procedure of four-point loading using eqn (19) and load-point deflection (Δ) should be used.

Conclusion

A novel method of flexural creep analysis has been developed to calculate the tensile creep rate in a simple way. The calculated tensile creep data are compared with experimental tensile creep data on the same ceramic materials. Based on a few assumptions about flexure creep, only the displacement rate, invariant with time in the secondary mode of creep, and beam deflection in four-point bending are needed to calculate the tensile creep rate. After obtaining the creep-induced tensile stress that corresponds to the applied tensile stress in the steady state of secondary creep, the tensile creep rate is compared with experimental creep data. These data show a reasonably good agreement for Al_2O_3 and Si_3N_4 ceramics. Therefore, the flexural creep test can be used not only to obtain the tensile creep rate but

also to verify the accuracy of the tensile creep test data. Flexural creep tests are much less expensive and easier to conduct for ceramic materials than tensile creep tests.

References

1. Rosenfield, A. R., Shetty, D. K. & Duckworth, W. H., Estimating tensile creep data from flexure data. *J. Am. Ceram. Soc.*, **69**[5] (1986) C108–9.
2. Carroll, D. F., Chuang, T. J. & Weiderhorn, S. M., A comparison of creep rupture behavior in tension and bending. *Ceram. Eng. Sci. Proc.* **9**[7–8] (1988) 635–42.
3. Chuang, T. J. & Weiderhorn, S. M., Damage-enhanced creep in a siliconized silicon carbide: mechanics of deformation. *J. Am. Ceram. Soc.*, 7[7] (1988) 595–601.
4. Talty, P. K. & Dirks, R. A., Determination of tensile and compression creep behavior of ceramic materials from bend tests. *J. Mater Sci.*, **13** (1978) 580–6.
5. Chuang, T. J., Estimation of power-law creep parameters from bend test data. *J. Mater. Sci.*, **21** (1986) 165–75.
6. Hollenberg, G. W., Terwilliger, G. R. & Gordon, R. S., Calculation of stresses and strains in four-point bending creep tests. *J. Am. Ceram. Soc.*, **54** (1971) 196–9.
7. Lin, H. T. & Becher, P. F., Creep behavior of a SiC-whisker reinforced alumina. *J. Am. Ceram. Soc.*, **73** (1990) 1378–81.
8. Krause, R. F. Jr, Observed and theoretical creep rate for an alumina ceramic and a silicon nitride ceramic in flexure. *J. Am. Ceram. Soc.*, **75**[5] (1992) 1307–10.
9. Ferber, M. K., Jenkins, M. G. & Tennery, V. J., Comparison of tension, compression and flexure creep for alumina and silicon nitride ceramic. *Ceram. Eng. Sci. Proc.*, **11**[7–8] (1990) 1028–45.
10. Jou, Z. C. & Virkar, A. V., High temperature creep and cavitation of polycrystalline aluminum nitride. *J. Am. Ceram. Soc.*, **73**[5] (1990) 1928–35.
11. Frett, T., Keller, K. & Munz, D., An analysis of the creep of hot pressed silicon nitride in bending. *J. Mater. Sci.*, **23** (1988) 467–74.
12. Dryden, J. R. & Watt, F., Re-distribution of stresses during creep-bending of grain boundary sliding materials. In *Proceedings of Surfaces and Interfaces in Ceramic and Ceramic–Metal Systems. Mater. Sci., Res.*, **19** (1981) 105–13.
13. Lee, D. J. & Palley, I., Tensile creep in ceramics using four-point bending test. *KSME J.*, **8**[3] (1994) 325–31.